Published in: Engineering Structures (2022), vol. 252, 113603
DOI: 10.1016/j.engstruct.2021.113603
Status: Postprint (Author's version)

DESIGN RECOMMENDATIONS FOR THE STABILITY OF TRANSMISSION STEEL LATTICE TOWERS

Marios-Zois Bezas

Steel and Composite Construction, UEE Research Unit, Liège University, Belgium – School of Civil Engineering, Institute of Steel Structures, National Technical University of Athens, Athens, Greece.

Jean-Pierre Jaspart

Steel and Composite Construction, UEE Research Unit, Liège University, Belgium.

Ioannis Vayas

School of Civil Engineering, Institute of Steel Structures, National Technical University of Athens, Athens, Greece.

Jean-François Demonceau

Steel and Composite Construction, UEE Research Unit, Liège University, Belgium.

Abstract. Lattice towers are extensively built in Europe and worldwide to serve telecommunication or power transmission purposes. Their members are usually made of equal leg angle profiles that are bolted at their extremities. Such types of towers are mainly designed to EN 1993-3-1 and EN 50341-1, based on a first-order linear elastic structural analysis of a truss structure. In this paper, an assessment of the current design approach is performed, where the tower has been simulated with a full non-linear finite element software, considering relevant imperfections as well as geometrical and material non-linearities. The importance of the second order effects in the analysis is underlined while the existence of an instability mode not properly covered directly by the norms, and usually therefore not checked, is highlighted. Two analytical models for the prediction of the critical load of this buckling mode are proposed and validated numerically. Both proposed models are rather easy to apply and may fill the gap in the existing design recommendations for lattice towers.

Keywords. Transmission tower, Steel lattice tower, Angle cross-section, Stability of pylons, Eurocode 3 , Segment instability, Non-linear analysis.

1. Introduction

Lattice towers are extensively built in Europe and worldwide to serve telecommunication or power transmission purposes. Often such towers are installed in mountainous terrains with very limited access to heavy vehicles. Consequently, a lattice tower structural system, which may be transported and erected by light machinery and equipment, is almost the only possible solution. The in situ modular

Published in: Engineering Structures (2022), vol. 252, 113603
DOI: 10.1016/j.engstruct.2021.113603
Status: Postprint (Author's version)

construction of the tower is simplified using bolted connections and gusset plates. On the other hand, lattice towers need more ground space compared to cylindrical, octagonal or similar shell-type systems. However, ground space is plentifully available in remote places outside the densely populated regions in most of the European countries. Therefore, lattice towers are used as the main structural system for telecommunication and power transmission.

The members of such towers are frequently composed of equal leg angle sections that are often preferred to tubular sections due to their easier connection that results in a simpler erection, a requirement set by most telecommunication or power providers. Angles sizes range from light to heavy profiles made of regular or high strength steel grades. Appropriate long-life corrosion protection is ensured with application of angles, since all angle sizes are fully amenable to hot dip galvanizing in contrast to several other types of open or closed sections.

Steel lattice towers are generally designed to Eurocodes and in particular to EN 1993-3-1 [1], in combination with EN 1993-1-1 [2] providing general rules, and EN 1993-1-8 [3] providing rules for connections. But in the specific field of overhead electrical lines exceeding 1 kV, lattice transmission towers are also designed to the CENELEC standard EN 50341-1 [4] which provides rules sometimes diverging from those proposed in the Eurocodes. Moreover, EN 50341-1 allows design by full scale testing. However, it draws design conclusions from a single test comparing the ultimate load achieved in the test with the corresponding one from calculations, neglecting the fact that the results of an individual test are influenced by potential material overstrength, strain hardening or other parameters, the values of which are associated with statistical uncertainties. Consequently, it does not touch reliability issues as it is done in the structural Eurocodes, in accordance with EN 1990 [5].

In all these normative documents, the tower is modelled as a simple truss structure where all the steel element connections are considered as hinged. Such models do not adequately reflect the actual tower behaviour of the structure, as loads and especially wind ones are directly imposed on the entire member length and introduce bending moments in members. Additionally, truss models induce more flexibility in the system and might lead to erratic modal vibration frequencies and dynamic wind effects. Furthermore, the design of lattice towers is classically carried out through a first order linear elastic analysis, neglecting the significant second order effects developing in these structures. It is therefore inconsistent and unsafe to perform member design by neglecting moments due to both local and overall loading, as well as the second order effects, as it is recommended by the norms and usually done in practice.

Extensive research has been carried out to study the modelling, the response and the failures of lattice towers. Klinger et al. [6] analysed the forensic expert reports written further to the failure of lattice towers which had been designed in accordance with the available norms; he proceeded to extensive materials investigations, mechanical testing of original components and specimens and estimations for the real wind and snow loads and their combinations. Albermani et al. [7] have studied the structural behaviour of the transmission towers through full non-linear analysis and compared them with full scale tests. The influence of the selected element (truss or beam) in the final response of the tower has been reported also by da Silva et al. [8]. Jiang et al. [9] investigated the modelling of the bolted connections and validated their response through available in the literature tests, while

Published in: Engineering Structures (2022), vol. 252, 113603
DOI: 10.1016/j.engstruct.2021.113603
Status: Postprint (Author's version)

Kitipornchai et al. [10] examined the effect of bolt slippage on the ultimate behaviour of lattice structures. A collection and critical review of full-scale tests on lattice towers as well as practical advice for conducting future tests are reported in Ref. [11]. Finally, most recent research on this topic has been made by Vlachakis et al. [12], where four experimental large-scale tests on angle section lattice towers subjected to pushover loading have been performed; the experimental tests are recalculated through the Eurocode 3 provisions which seems to be very conservative and need to be improved.

In this paper, a typical electric transmission steel lattice tower made of angle section members has been selected. The tower has been designed by means of a commercial software in accordance with the current normative requirements, based on a first-order linear elastic structural analysis of a truss structure. For the assessment of the design, the tower has been simulated with a full non-linear finite element software using beam elements, considering relevant imperfections as well as geometrical and material non-linearities. In these simulations, every single member has been properly modelled, in terms of orientation and eccentricities at its extremities. The importance of considering second order effects in the analysis is underlined. Then, the existence of an instability mode not properly covered by the European normative documents, is highlighted. This buckling mode, named by the authors as segment instability, is associated with the buckling of more than one member forming a segment. Although several segment failures have been studied experimentally and numerically by Rao et al. [13], the one described in the present paper is not addressed. Subsequently, for this specific buckling mode, two analytical models for the prediction of the critical load are proposed, followed by their numerical validation, in order to complement existing code provisions. Finally, comparisons with the existing norms, but also with the new forthcoming version of EN 1993-3-1, namely prEN 1993-3-1 [14] are made. The numerical and analytical studies are part of the European-funded RFCS project called ANGELHY [15] involving National Technical University of Athens (NTUA - coordinator), CTICM (France), Li`ege University as well as ArcelorMittal, COSMOTE and SIKA companies.

2. Details of the selected tower

A Danube tower type has been selected – its geometry is shown in Fig. 1 – which is the most typical tower form of transmission lines in Europe. In the framework of the present study, only a suspension lattice steel tower is considered and not the entire transmission line. The tower is supposed to be erected in the Erzgebirge in Saxony (Germany) and is part of a straight transmission line; the location of the tower is used only for the evaluation of the normative wind loads acting on it. The wind span between two successive towers is 350 m, while the weight span, due to significant height differences, equals 1,5·350 = 525 m [16]. The tower supports two 380 kV circuits on each side, while on its top, it carries one single earth wire for lightning protection. The conductors and the earth wire are made of steel fibres enveloped by several fibres of aluminium. Based on EN 50182 [17], a "94-AL1/15-ST1A" and a "264- AL1/34-ST1A" have been selected for the earth wire and the conductors respectively. Each conductor is connected to a 5 m suspension insulator (Quadri*Sil Insulator of Hubbell company). All the members of the tower are angle profiles made of steel grade S355J2.

Published in: Engineering Structures (2022), vol. 252, 113603
DOI: 10.1016/j.engstruct.2021.113603
Status: Postprint (Author's version)

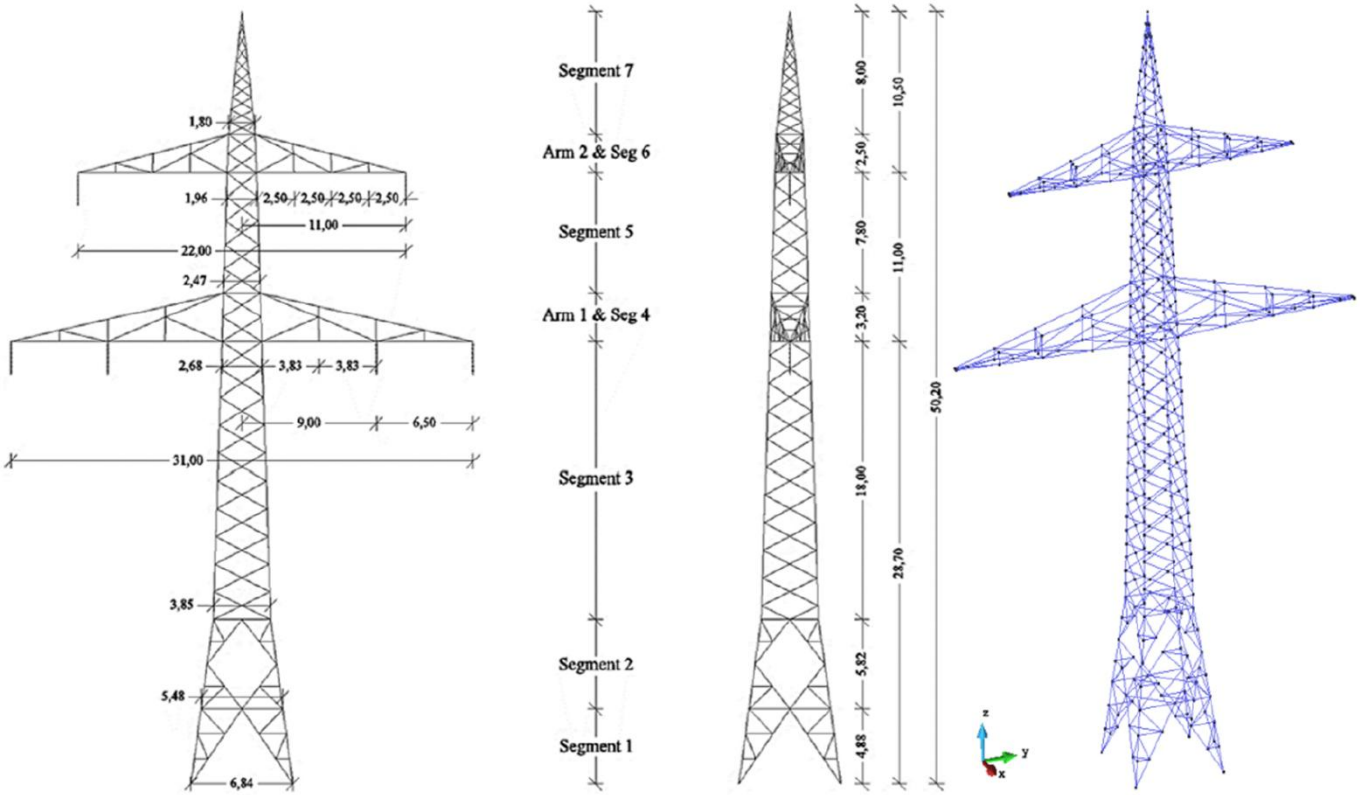

Fig. 1. Geometry of the studied Danube tower and 3-D model from FINELG software.

The initial design has been done by TOWER finite element software [18], which is dedicated to the design of transmission and telecommunication steel lattice towers according to different international standards. The tower is initially designed under gravity and wind loads following the recommendations and requirements of EN 50341-1 and EN 50341-2-4 [19]. The design is carried out through a first order linear elastic analysis of a truss structure. The eccentricities of the connections are not modelled, but their influence is considered via effective non- dimensional slenderness in the member buckling checks. More details about the design of the tower (profiles, load cases, numerical model etc.) can be found in Ref. [20].

3. Description of the numerical model

Beam finite elements with 7 degrees of freedom have been used in the FINELG finite element software [21], as plate buckling phenomena in the angle legs are not to be contemplated. The model of the tower is represented in Fig. 1. It is worth noting that FINELG has been already successfully used in the past to simulate a lattice tower [22]. More recently the software has been validated through comparisons of experimental tests on isolated angle members [23] and full-scale test on pylons [24].

Every element/beam is modelled with its appropriate eccentricity, rotation and orientation in order to simulate the reality as closely as possible. At the level of a global analysis, the bolted connections

Published in: Engineering Structures (2022), vol. 252, 113603
DOI: 10.1016/j.engstruct.2021.113603
Status: Postprint (Author's version)

between the diagonals and tower legs as well as the splices in the tower legs are not considered directly in the model. However, the self-weight of gusset plates and bolts was considered by multiplying the dead weight of the tower by the factor of 1,20; this approach has been used also for the initial design of the tower, as it is a widely done in practice. The connection behaviour has been simulated through appropriate hinges/ constraints at the ends of the elements. The main tower legs are considered as continuous over their total length while the primary and secondary bracing members and the horizontal members are considered as pinned at their ends. For those members, all the rotations are free, except the torsion about the beam axis which is blocked. All the other DOF are blocked too. The legs are assumed as pinned at their base (but the rotation that leads to torsion of the exterior leg is blocked).

All the members of the tower are made of steel grade S355J2. Two cases are considered in terms of material law: a linear elastic one and a non-linear perfectly plastic one. Nominal values for the material properties are used (E = 210.000 MPa, v = 0,3 and ρ = 7850 kg/m^3), while the yield stress is taken equal to 345 MPa. For each element, residual stresses resulting from hot-rolling are considered in material non-linear analyses; the pattern is in accordance with Ref. [25]. Furthermore, for the 2nd order analyses where initial imperfections have been applied, those are in accordance with the 1st instability mode, calibrated so as to reach an amplitude of L/1000 (L is the length of the member/segment where instability occurs).

Twelve different load combinations are indicated in EN 50341, regarding the wind direction (with angle 0°, 45° and 90° with the cross arms) and the definition of the actions (favourable/ unfavourable) have been considered for the initial design of the tower. Amongst them, three representative cases have been here selected for the assessment of the design, which correspond to unfavourable actions (for the determination of the axis, see Fig. 2):

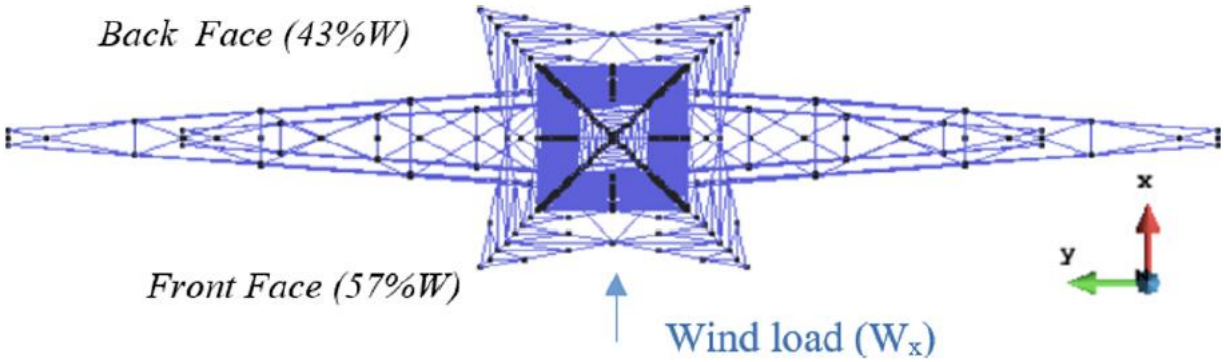

Fig. 2. Definition of wind direction.

X direction: gravity loads (G) and wind forces perpendicular to the cross arms (W_x).

Y direction: gravity loads (G) and wind forces in direction of the cross arms (W_y).

XY$_{45}$ direction: gravity loads (G) and wind forces in 45° with Y axis ($W_{xy,45}$).

Published in: Engineering Structures (2022), vol. 252, 113603
DOI: 10.1016/j.engstruct.2021.113603
Status: Postprint (Author's version)

The self-weight of the tower itself is calculated automatically by the software and multiplied by the factor 1,20 as already said. The self- weight of the conductors and the earth wire are evaluated according to Ref. [17]. The wind loads on the conductors and the earth wire, as well as their self-weight, are calculated separately and introduced in the model as point loads without considering any load eccentricity. Longitudinal loads in the conductors are not considered since it is a suspension tower in a straight line (as the conductors are simply suspended from the tower, the mechanical tension being the same on each side).

The calculation of the wind loads on the tower is based on EN 1993- 3-1 and EN 1991-1-4 [26]. The tower is subdivided into several segments (see Fig. 1) and, for each one, a mean wind load is evaluated for the three considered directions. Then, the mean wind load in each direction is distributed on the front and back face of the tower. It is assumed that 57% of the total wind load is acting on the front face of each segment, while 43% on the back face (see Fig. 2). On each beam element of the tower, the wind load is acting normal to its face with a constant distributed beam value. The wind loads on the conductors, the earth wire and the insulators are based on EN 1993-3-1.

It should be said that the wind loads have been evaluated with different standards in the different software, TOWER and FINELG. Although there are some differences between the standards, the total acting wind force per direction does not differ so much (about 4,2%); according to EN 50341-2-4 wind loads are bigger for the tower's body but are smaller for the conductors. However, the way that the loads are applied on the tower (i.e constant distributed loads along the beams in FINELG in comparison with the concentrate forces at the nodes used in TOWER) influences more the response of the tower; and for sure the assumption made in FINELG is much closer to the reality.

Same safety load factors will be used for the applied loads as the ones used in the initial design of the pylon, i.e $\gamma_G = {}_{\gamma W} = 1{,}35$ for unfavourable actions according to EN 50341-2-4. For all the analysis, the gravity loads are first applied and then wind loads are increased $[1{,}35G + \alpha(1{,}35\ W)]$ until failure of the tower occurs. This load sequence simulation is closer to the reality. More details about the simulation with FINELG software, as well as a comparison of both FINELG and TOWER models in the elastic range (self-weigh, maximum displacements and total stiffness) can be found in [27,28].

4. Numerical results

In order to investigate the tower response and validate the initial design method, different type of analyses have been performed by means of FINELG and the results are presented in the next paragraphs.

4.1. ELASTIC INSTABILITY ANALYSIS

The critical load multipliers are summarised in Table 1. The deformation shape of the first instability mode for wind loads acting on X direction is shown in Fig. 3, while for wind loads acting on Y and XY_{45} direction the shape is the same and illustrated in Fig. 4. For the first case (Fig. 3), instability occurs at the front horizontal bar of the horizontal level at the bottom of the lower cross-arms.

Published in: Engineering Structures (2022), vol. 252, 113603
DOI: 10.1016/j.engstruct.2021.113603
Status: Postprint (Author's version)

The instability mode observed here (Fig. 4) is named by the authors "segment instability" and is further investigated in Section 5.

Table 1
Results from elastic instability analysis.

Load combination	Load factor α_{cr}	Type of instability
X direction	3,056	Member
Y direction	1,015	Segment
XY_{45} direction	1,783	Segment

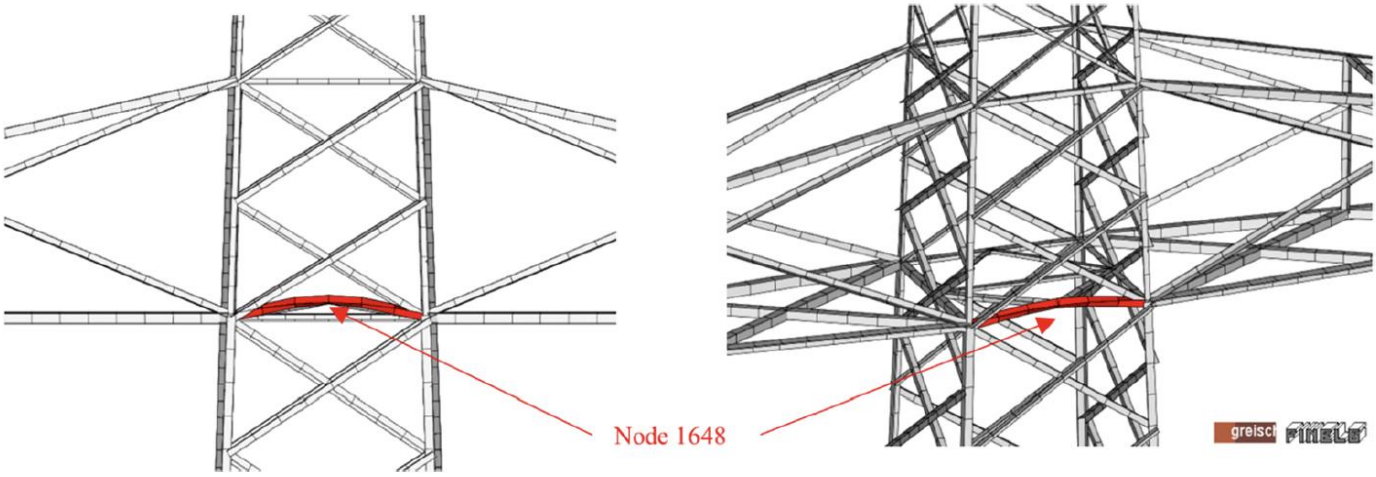

Fig. 3. First instability mode for load combination $1{,}35G + \alpha_{cr}1{,}35W_x$.

Published in: Engineering Structures (2022), vol. 252, 113603
DOI: 10.1016/j.engstruct.2021.113603
Status: Postprint (Author's version)

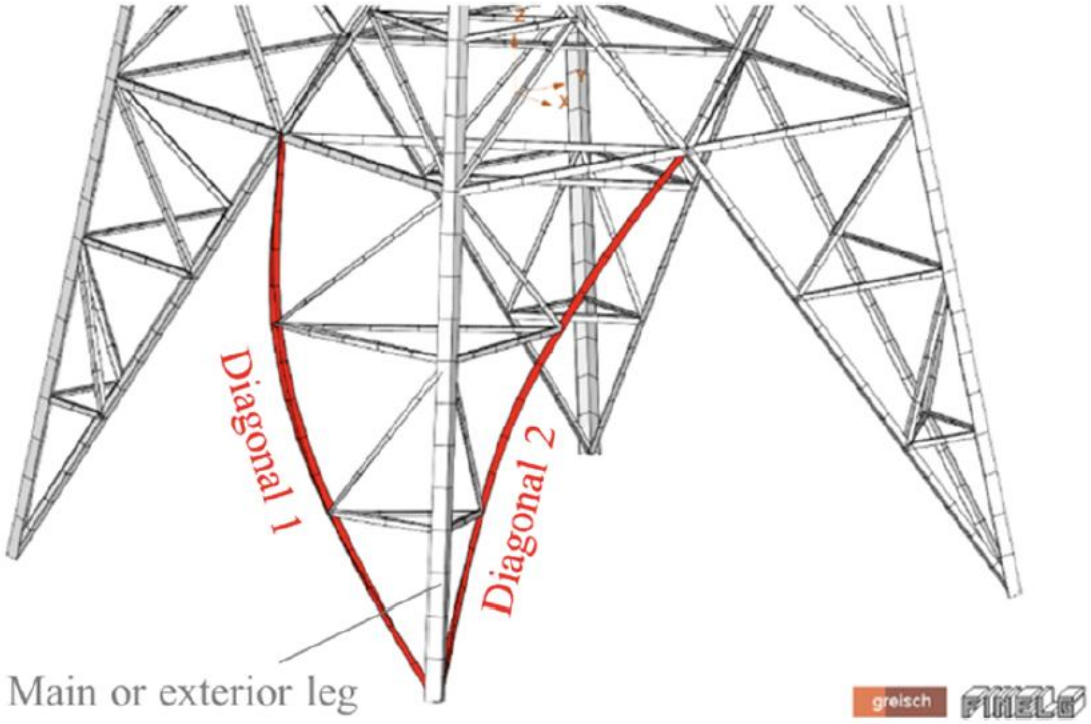

Fig. 4. First instability mode for load combination $1{,}35G + \alpha_{cr}1{,}35W_y$ and $1{,}35G + \alpha_{cr}1{,}35\ W_{45}$.

4.2. SECOND ORDER ELASTIC ANALYSES

Geometrically non-linear elastic analyses with elastic material law without considering initial imperfections have been performed. The results are summarized, for each wind direction, below.

For the load combination $1{,}35G + \alpha_{cr,nl}1{,}35W_x$, the load–displacement curve is reported in Fig. 5. The abscissa represents the global vertical displacement (see Fig. 1 for the definition of the axis), while the horizontal dot line corresponds to the critical load multiplier resulting from the elastic buckling analysis. For both analyses, instability occurs in the same beam (see Fig. 3). It is a priori surprising to see that the critical load obtained by the instability analysis ($\alpha_{cr} = 3{,}056$) is significantly higher than the maximum load factor obtained by the geometrically non-linear elastic analysis ($\alpha_{cr,nl} \approx 1{,}71$). When checking the internal forces at the middle node of the beam (node 1648) in both cases (see Table 2), one realises that the failure occurs for two different triplets of relative axial force and bending moments. Indeed, in the second order linear elastic analyses, the second order effects are significantly influencing the internal forces in the members. In a member with a double- symmetrical section, this would have no effect on the member critical resistance, but this is not the case for angle sections, what extra investigations on isolated members have shown. This explains why the non-linear load multiplier is higher than the one obtained through an elastic instability analysis.

Published in: Engineering Structures (2022), vol. 252, 113603
DOI: 10.1016/j.engstruct.2021.113603
Status: Postprint (Author's version)

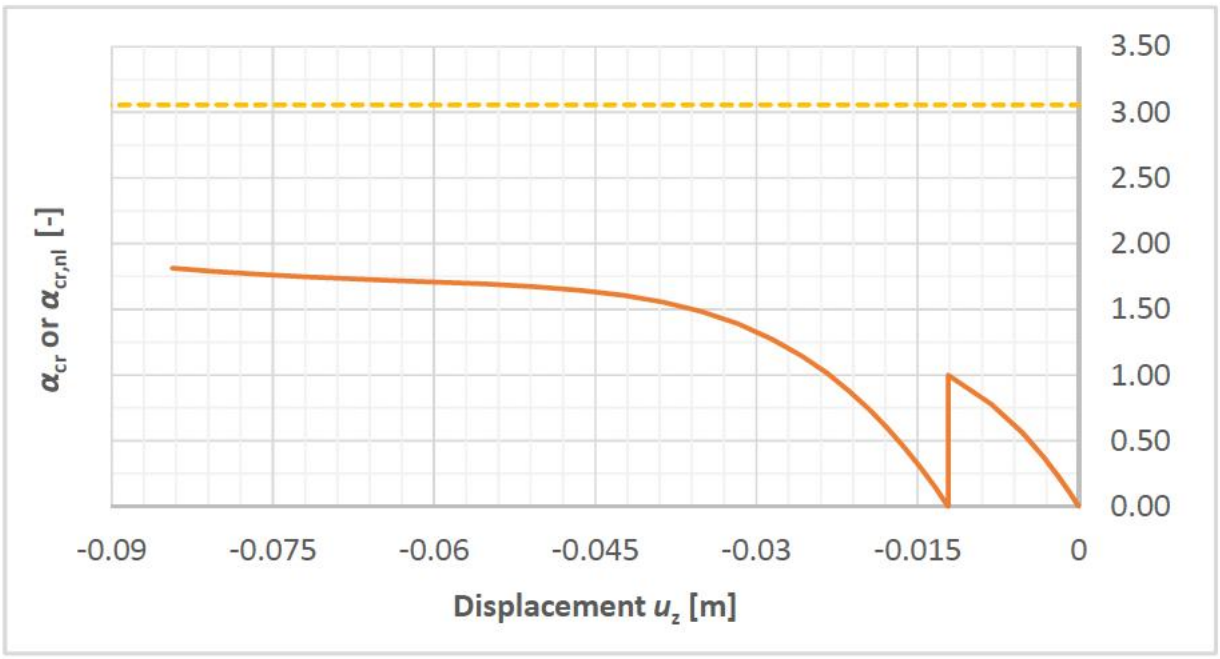

Fig. 5. Displacement u_z versus load factor for different types of analyses - wind perpendicular to the arms (X direction).

Table 2
Internal forces at node 1648, for the two analyses.

Internal forces	Elastic instability analysis	2nd order linear elastic analysis without initial imperfections
Axial N [kN]	−266,92	−177,10
Torsion M_T [kNm]	0,05	0,413
Bending M_{bu} [kNm]	3,56	10,19
Bending M_{bv} [kNm]	−0,24	−5,08
Load factor α_{cr} or $\alpha_{cr,nl}$	3,06	1,71

When the wind forces acting on Y direction, a segment instability again appears, as shown in Fig. 4. The graph in Fig. 6 shows the horizontal displacement u_x (direction of global X axis – Fig. 1) at the middle of diagonal 2 versus the load factor. The horizontal dot line represents the critical load multiplier obtained from the elastic instability analysis. The difference between the critical instability load factor and the maximum one reached through a 2nd order linear elastic analysis, that is about

Published in: Engineering Structures (2022), vol. 252, 113603
DOI: 10.1016/j.engstruct.2021.113603
Status: Postprint (Author's version)

$\alpha_{cr,nl} \approx 0,68$, could again be explained by the different loading situations (relative axial force and bending moments) in the critical beams.

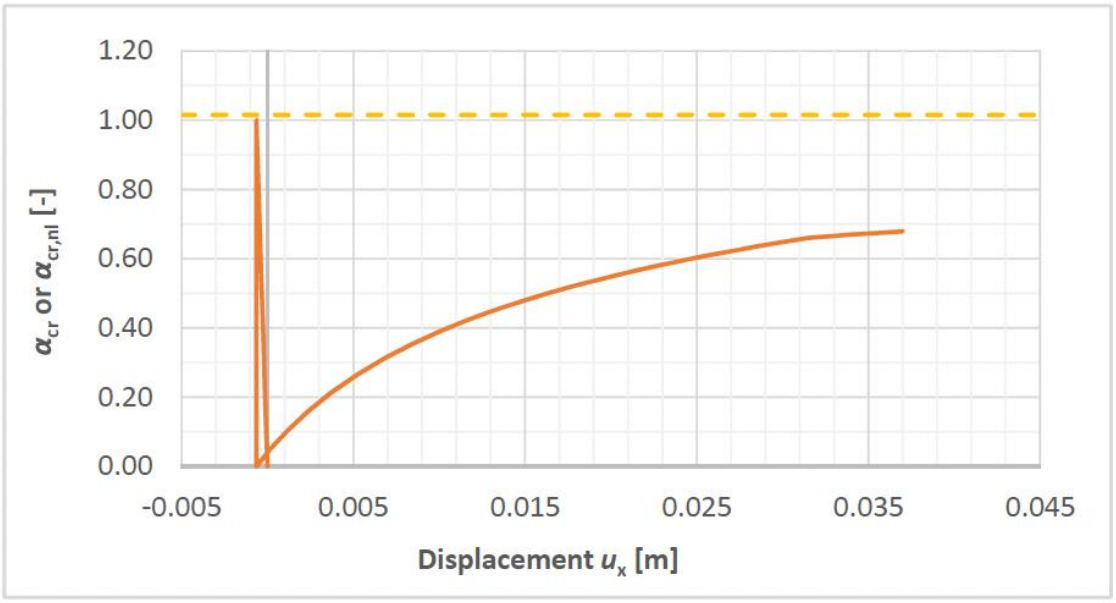

Fig. 6. Displacement u_x versus load factor for different types of analyses - wind parallel to the arms (Y direction).

As before, when wind forces act in the XY_{45} direction, a segment instability appears (Fig. 4) and the load–displacement curve is shown in Fig. 7. The critical load multiplier obtained from the elastic instability analysis equals $\alpha_{cr} = 1,783$ and is represented by the horizontal dot line, while the maximum load factor reached through the 2nd order linear elastic analysis is about $\alpha_{cr,nl} \approx 0,84$. The difference between both load factor multipliers has already been explained in the previous paragraphs.

Published in: Engineering Structures (2022), vol. 252, 113603
DOI: 10.1016/j.engstruct.2021.113603
Status: Postprint (Author's version)

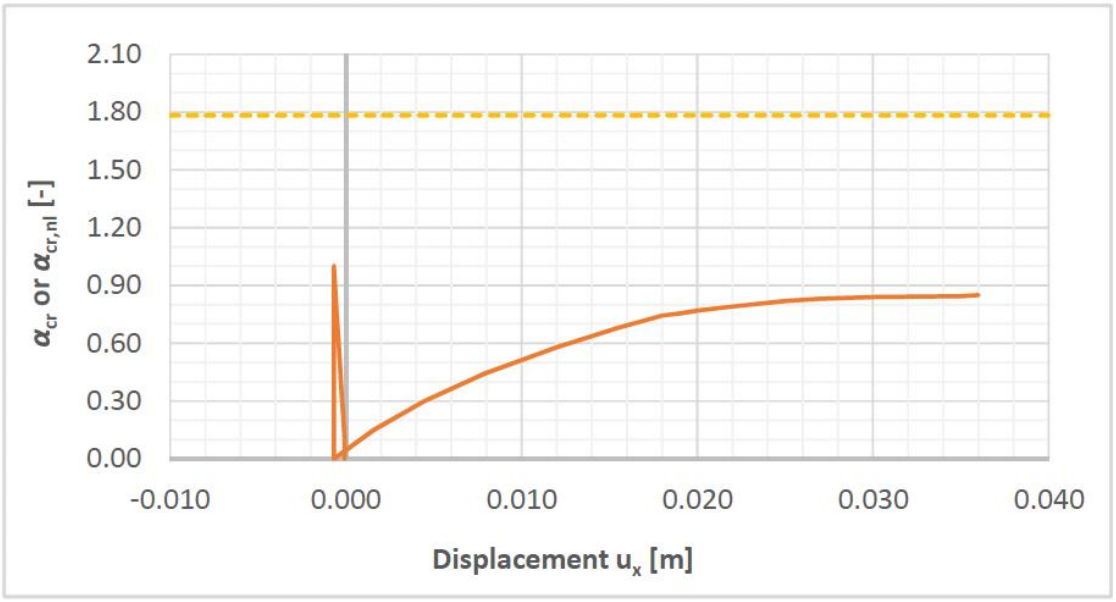

Fig. 7. Displacement u_x versus load factor for different types of analyses - wind with 45° to the arms (XY_{45} direction).

4.3. FULL NON-LINEAR ANALYSES

The validation of the initial design requires a full non-linear analysis, considering an elastic-perfectly plastic material, distributions of residual stresses and an initial imperfection of the structure in accordance with the 1st instability mode.

Fig. 8 represents the vertical displacement u_z (direction of global Z axis) at the node 1648 versus the load factor for the load combination $1{,}35G + \alpha_u 1{,}35W_x$. The failure occurs in the same beam as in the previous analyses. The load factor (α_u = 1,17) for this load combination is bigger than 1,0 with comparison to the design factored loads. As a result, the initial design appears to be safe for this load combination. Furthermore, it is observed that the tower remains elastic for load factors $\alpha_u \leq 1{,}0$, so confirming the TOWER design assumptions.

Published in: Engineering Structures (2022), vol. 252, 113603
DOI: 10.1016/j.engstruct.2021.113603
Status: Postprint (Author's version)

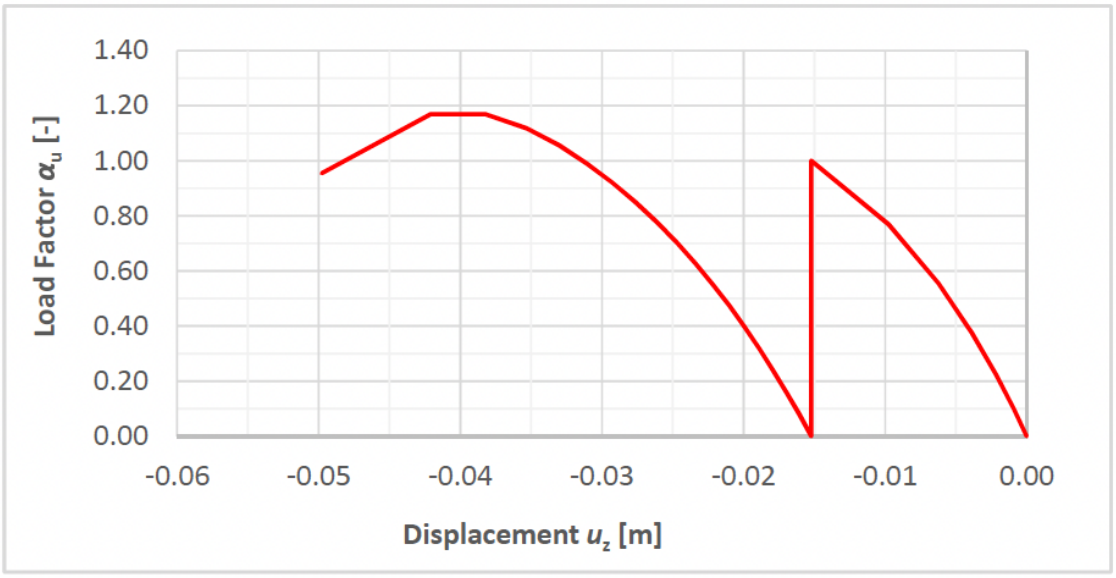

Fig. 8. Displacement versus ultimate load factor – $1{,}35G + 1{,}35W_x$ (X direction).

Fig. 9 shows the horizontal displacement u_x (direction of global X axis) at the middle of diagonal 2 versus the load factor, for the load combination $1{,}35G + \alpha_u 1{,}35W_y$. It can be seen that the load factor is about $\alpha_u \approx 0{,}66$. Contrary to what is seen before, the maximum load factor remains here far lower than 1,0. The initial design of the tower by TOWER software for this direction is therefore seen as insufficient and unconservative. This may be explained by the development, in reality, of an instability mode in one of the main tower legs, called "segment instability" and which is not covered by TOWER; but more importantly, also not addressed directly by the reference European normative documents EN 1993-3-1 and EN 50341 (see Section 5.3).

Similarly, for the load combination $1{,}35G + \alpha_u 1{,}35W_{XY45}$, the ultimate load factor is about $\alpha_u \approx 0{,}82$. Thus, the initial design is unsafe, again due to the development of the segment instability failure.

Published in: Engineering Structures (2022), vol. 252, 113603
DOI: 10.1016/j.engstruct.2021.113603
Status: Postprint (Author's version)

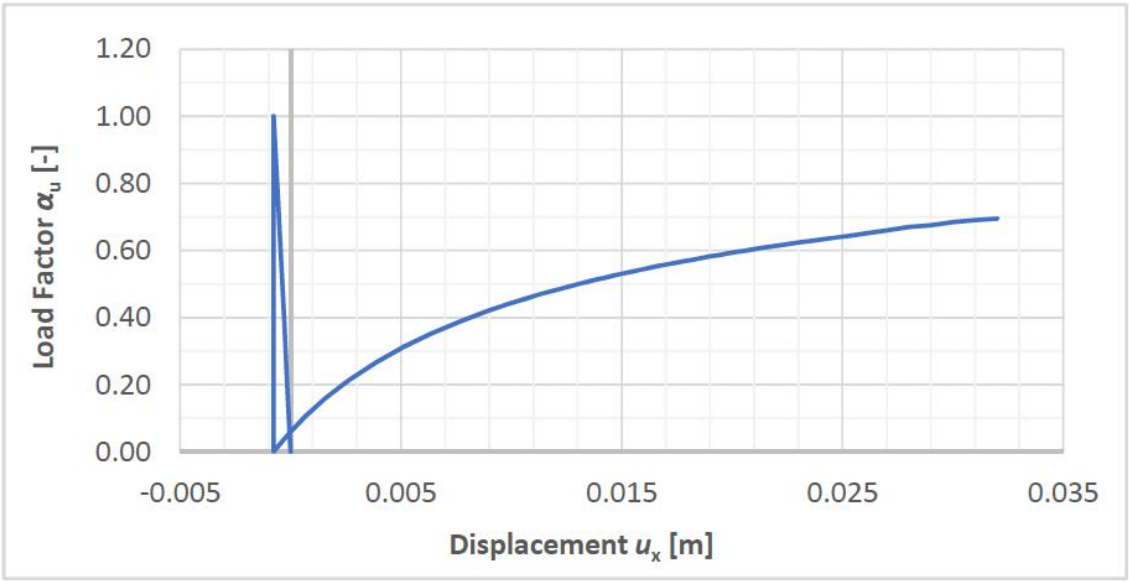

Fig. 9. Displacement versus ultimate load factor – $1{,}35G + 1{,}35Wy$ (Y direction).

5. The segment instability mode

A "segment instability" is defined as an instability mode associated to the buckling of more than one member forming a segment. In the paper, the instability is associated to the buckling of the two diagonals of a leg of a transmission tower (see Fig. 4) and therefore could also be named "leg-segment instability". More precisely, the leg consists of three vertically orientated members: the main or exterior leg and the two diagonals (1 & 2) that are connected with a number of horizontal beams and bracing members forming "triangles". In fact, each of the two diagonals and the exterior leg constituting the segment are stable individually and can resist to the applied maximum forces, as they have been initially designed for that. However, the simultaneous buckling of the diagonals over the whole leg height, involving a longitudinal rotation of the main leg member, represents a buckling mode which has been seen to be relevant in various usual design situations.

Fig. 10 shows a horizontal cut in the leg and indicates how the constitutive elements deform in the instability mode. The diagonals move laterally and bend about an axis parallel to one of their angle legs (geometrical axis) while the exterior leg rotates about its longitudinal axis. The elements which form the "horizontal leg triangles" do not undergo any deformation; they are just translated.

Two models, a simplified one and a refined one, to predict the critical loads of the segment instability mode are first presented. Then, a model to predict the buckling resistance of the leg is described.

Published in: Engineering Structures (2022), vol. 252, 113603
DOI: 10.1016/j.engstruct.2021.113603
Status: Postprint (Author's version)

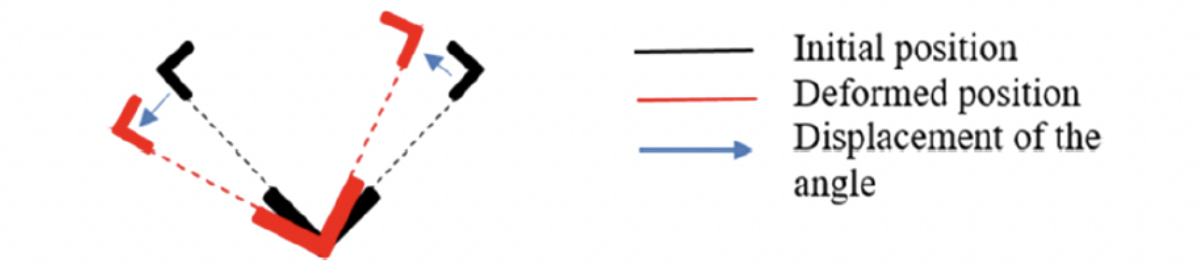

Fig. 10. Deformation of the members through a horizontal cut in the leg.

5.1. PROPOSED ANALYTICAL MODELS

5.1.1. SIMPLIFIED MODEL

The equivalent model illustrated in Fig. 11 has been built, in order to represent physically what is observed in the leg. The two parallel vertical members represent the two diagonals and the horizontal pinned members, the elements forming the horizontal leg triangle. Both diagonals are assumed to be made of the same profile, as it happens in practise in most of the cases. The extremities of the vertical members are assumed to be hinged; this is what is expected at the foundation level, while the very small restraining effect resulting from the actual continuity of the diagonals at the top is neglected. The modal deformed shape of the system is illustrated on the right side of Fig. 11.

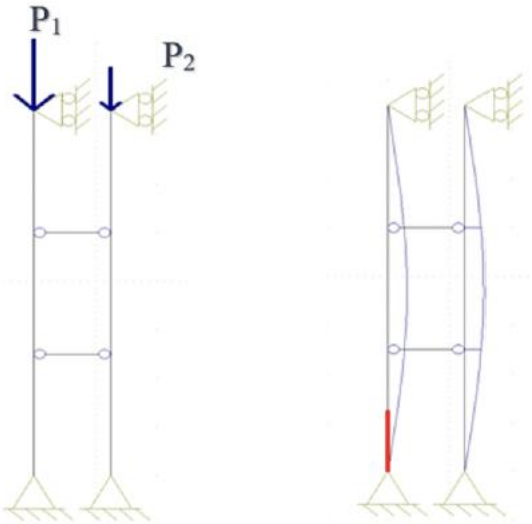

Fig. 11. Equivalent model of the leg (left) and modal deformed shape (right).

For the simplified model, the critical load may be given by the following equation:

$$N_{cr} = \frac{2\pi^2 E I_y}{L^2} \qquad (1)$$

where,

Published in: Engineering Structures (2022), vol. 252, 113603
DOI: 10.1016/j.engstruct.2021.113603
Status: Postprint (Author's version)

I_y is the moment of inertia about y-y geometrical axis of the diagonal's cross-section;

L is the buckling length of the diagonal; E is the modulus of elasticity.

Thus, the critical load multiplier may be determined as follows:

$$a_{cr} = \frac{N_{cr}}{P_1 + P_2} \tag{2}$$

where,

N_{cr} is the critical load given by Eq. (1);

P_1, P_2 are the compression forces at the diagonals (see Fig. 11);

This model is independent of the number of horizontal "rigid triangles", and therefore may be generally used for segments with pyramidal configuration.

5.1.2. REFINED MODEL

In the proposed refined model, the beneficial effect of the torsional stiffness of the exterior leg, which has been disregarded in the simplified one, is considered. When the segment instability occurs, the exterior member is assumed to be individually stable. If it would not be the case, then the buckling of the exterior leg determines the failure and limits the pylon resistance. Therefore, considering the fact that the buckling resistance of an individual member in compression follows a flexural mode and not a torsional one, it can be reasonably assumed that the axial force in the exterior leg is not influencing its torsional stiffness.

When the leg instability develops, the exterior member is activated in torsion at the 1/3 and the 2/3 of the member length (L_{ext}) where the "triangles" are here assumed to be located. The first step consists in the evaluation of the torsional restraint offered by the rigidity of the exterior leg member in torsion. In this model, it is assumed that the torsion of the exterior leg is blocked at its extremities.

The torsional moment (see Fig. 12) can be evaluated as follows, considering that M_{T1} and M_{T2} are equal to M_T:

$$\varphi = \int_0^{\frac{L_{ext}}{3}} \frac{M_T}{C} dx \Rightarrow M_T = \frac{3C}{L_{ext}} \varphi \tag{3}$$

Published in: Engineering Structures (2022), vol. 252, 113603
DOI: 10.1016/j.engstruct.2021.113603
Status: Postprint (Author's version)

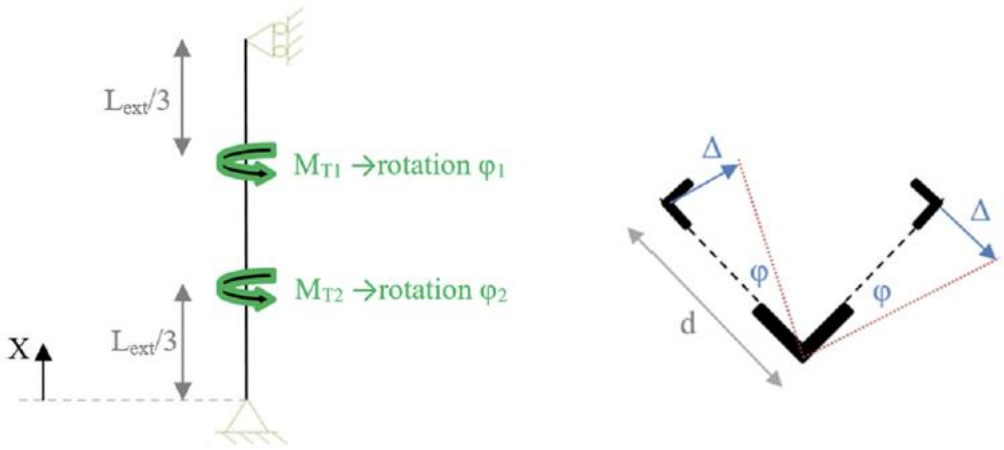

Fig. 12. Schemes for the calculation for the torsional restraint brought by the exterior member.

The torsional rigidity *C* of the cross-section is approximately equal to:

$$C = \frac{G}{3}\sum hb^3 = \frac{G}{3}\cdot 2\cdot(h-0,5t)t^3 \tag{4}$$

Then:

$$\left.\begin{aligned} M_T &= \frac{3C}{L_{ext}}\varphi \\ M_T &= 2Fd \end{aligned}\right\} \Rightarrow \frac{3C}{L_{ext}}\varphi = 2Fd \Rightarrow^{F=R\Delta} \frac{3C}{L_{ext}}\varphi = 2R\Delta d \Rightarrow^{\Delta=d\varphi} \frac{3C}{L_{ext}}\varphi = 2Rd^2\varphi \tag{5}$$

where *F* is a force applied at each diagonal in direction of *Δ* and which causes torsional moment at the exterior member of the leg ($M_T = 2F\cdot d$), while *R* is the lateral restraint of the diagonal ($R = F/\Delta$). By solving Eq. (5), the lateral restraint of the diagonal is obtained:

$$R = \frac{3C}{2L_{ext}}\cdot\frac{1}{d^2} \tag{6}$$

The torsional restraints evaluated at 1/3 or at 2/3 of the member length (where the rigid triangles act) are different as different values of *d* are met at these locations, what implies different values for M_{T1} and M_{T2} in Fig. 12 and invalidates de facto the use of Eq. (3). But, for sake of simplicity, the actual values of *R* at *L*/3 and at 2*L*/3 are substituted by a mean value of R_{mean} defined as follows:

$$R_{mean} = \frac{3C}{2L_{ext}}\cdot\frac{1}{n}\sum_{i=1}^{n}\frac{1}{d_i^2} \tag{7}$$

Published in: Engineering Structures (2022), vol. 252, 113603
DOI: 10.1016/j.engstruct.2021.113603
Status: Postprint (Author's version)

This is illustrated in Fig. 13. To simplify it further, both restraints are merged into a single one called K_T, as illustrated in the right sketch of Fig. 13. For this case, Gardner proposes in Ref. [29] an analytical expression of the critical load for a column of flexural inertia *I*:

$$N_{cr} = \frac{\pi^2 EI}{L^2} + \frac{3}{16} K_T L \text{ with } K_T < \frac{16\pi^2 EI}{L^3} \quad (8)$$

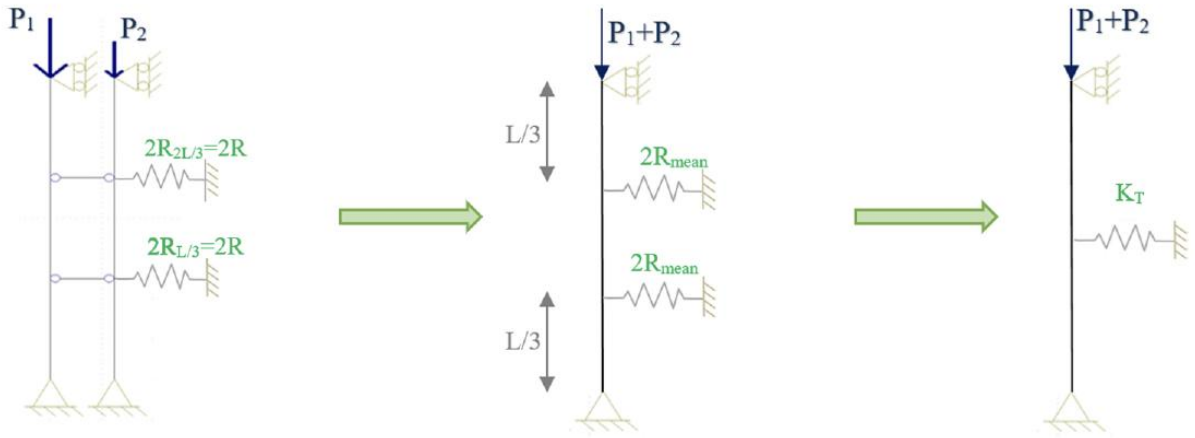

Fig. 13. Initial (left), intermediate (middle) and final (right) proposed design model.

If K_T reaches a value of $\frac{16}{L}\pi_{3^2}EI$, the column will buckle in the second eigenmode (two half sine waves); further increases of the K_T values will not produce a corresponding increase in the critical load. The column therefore effectively becomes restrained at its mid-height, and $N_{cr,2} = \frac{4\pi}{L^2}EI$ (see Fig. 14). In the specific case of pylons, the restraints remain quite low, and for sure much lower than $\frac{16}{L}\pi_{3^2}EI$.

Published in: Engineering Structures (2022), vol. 252, 113603
DOI: 10.1016/j.engstruct.2021.113603
Status: Postprint (Author's version)

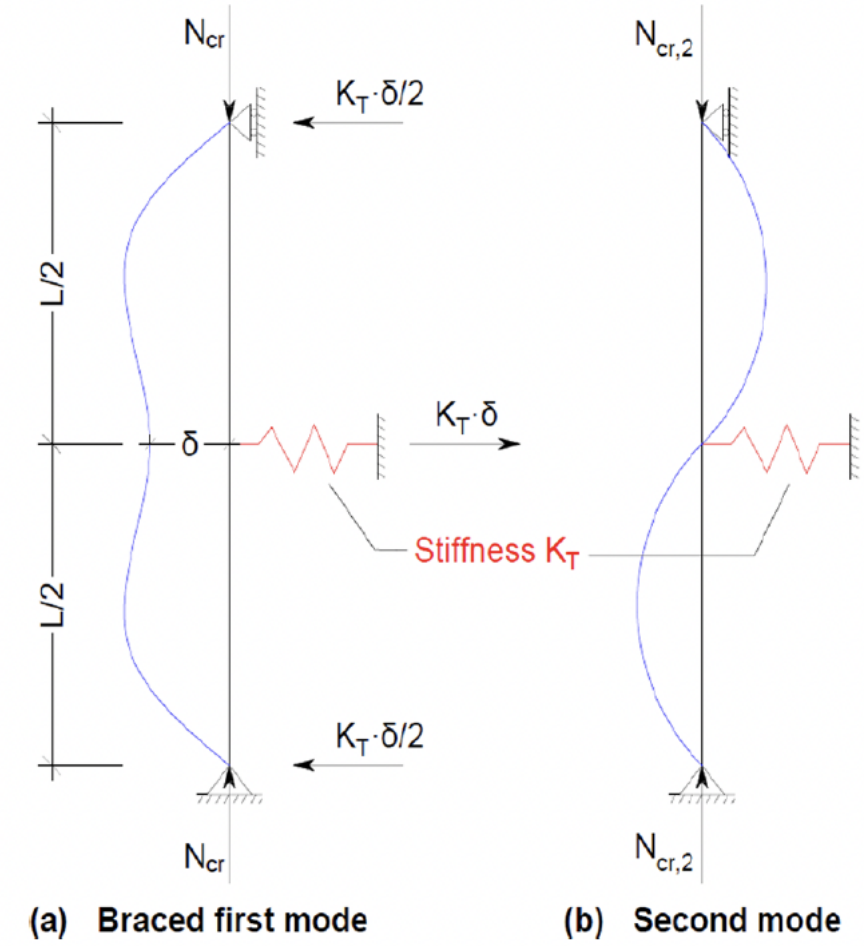

Fig. 14. Column with a single discrete restrain [29].

The determination of the spring stiffness K_T may be contemplated referring to the literature (p.474–475 of Ref. [30]), from which it may be deduced that for few discrete supports, the term $m\,{}_{EI}C/l^3$ is constant. In this expression, m is the number of zones of length $l = L/m$ separated by rigid triangles in the leg, $C = 2R_{mean}$ and $EI = 2EI_y$ where I_y is the value of the flexural rigidity of one diagonal.

$$m\frac{C}{EI}l^3 = const \Rightarrow \; m\cdot 2R_{mean}\cdot\left(\frac{L}{m}\right)^3 = 2\cdot K_T\cdot\left(\frac{L}{2}\right)^3 \tag{9}$$

This being, the equivalent spring stiffness K_T may be evaluated as follows:

$$K_T = \frac{4}{m^2}(2R_{mean}) \tag{10}$$

The critical load of the equivalent column may be given by:

$$N_{cr} = \frac{\pi^2 EI_{y,tot}}{L^2} + \frac{3}{16}K_T L \tag{11}$$

Published in: Engineering Structures (2022), vol. 252, 113603
DOI: 10.1016/j.engstruct.2021.113603
Status: Postprint (Author's version)

where,

$I_{y,tot}$ is the total moment of inertia about y-y geometrical axis of both diagonals (i.e $I_{y,tot} = 2I_y$);

L is the buckling length of the diagonal;

E is the modulus of elasticity;

K_T is the stiffness of the unique spring restraint, equal to $\frac{4}{m^2}(2R_{mean})$;

R_{mean} can be evaluated using Eq. (7);

m is the number of zones of length l in the leg ($l = L/m$ separated by rigid horizontal triangles in the leg); the accuracy of the formulae for K_T is sufficient for a value of $m \leq 6$ (i.e for maximum 5 horizontal rigid triangles in the leg);

d_i is the horizontal distance of the longitudinal axis of one diagonal from the longitudinal axis of the main leg, where i is the index for the horizontal level (see Fig. 12).

The critical load multiplier can be evaluated using Eq. (2), for this model too.

5.1.3. ULTIMATE RESISTANCE OF THE LEG

The ultimate buckling resistance of the leg may be determined by the current provisions of EN 1993-1-1, as follows:

$$N_{b,Rd} = \begin{cases} \chi \dfrac{A_d f_y}{\gamma_{M1}} & \text{for class } 1, 2 \text{ and } 3 \text{ profiles} \\ \chi \dfrac{A_{d,eff} f_y}{\gamma_{M1}} & \text{for class } 4 \text{ profiles} \end{cases} \tag{12}$$

where A_d and $A_{d,eff}$ is the gross and the effective area of the diagonal's cross-section respectively. The buckling reduction factor χ is determined as a function of the relative slenderness:

$$\overline{\lambda_{seg}} = \sqrt{\frac{2N_{pl}}{N_{cr}}} \tag{13}$$

where,

N_{cr} is the critical load of the segment determined by one of the proposed models (simplified or refined);

N_{pl} is the plastic design resistance of one diagonal ($N_{pl} = A_d f_y$).

The value of the buckling reduction factor χ can be determined from the European buckling curve d for any steel grade. It is suggested to safely use the lowest of the buckling curves due to the lack of studies showing that a higher one could be safely used.

Published in: Engineering Structures (2022), vol. 252, 113603
DOI: 10.1016/j.engstruct.2021.113603
Status: Postprint (Author's version)

5.2. NUMERICAL VALIDATION OF THE PROPOSED MODELS

The validation of the proposed formulae (simplified and refined) has first been achieved through comparisons to results obtained through 2D numerical simulations of the proposed models (illustrated in Fig. 11 and Fig. 13-right) by means of the OSSA2D software [31], and then through the use of the whole tower model, using FINELG software. As already explained in Section 3, FINELG has been validated through comparisons of experimental tests on towers; it is therefore prudent to rely on its use to validate the segment model. The reference codes for the constitutive elements of the tower leg simulated in FINELG are illustrated in Fig. 15, while details about the members are reported in Table 3.

For the refined model, the mean value of the lateral restraint R of the diagonals is

$R_{mean} = \frac{3C}{2L_{ext}} \cdot \frac{1}{n} \sum_{i=1}^{n} \frac{1}{d_i^2} = \frac{3 \cdot 1{,}69761 \cdot 10^{10}}{2 \cdot 5000} \cdot \frac{1}{2} \left(\frac{1}{913^2} + \frac{1}{1827^2} \right) = 3$, 82 N/mm. Consequently, the stiffness K_T of the spring is

$$\frac{4}{m^2}(2R_{mean}) = \frac{4}{3^2}(7,64) = 3,39 \text{ N/mm.}$$

By using the OSSA2D software and performing an elastic buckling analysis, the values of the critical load multipliers ($\alpha_{cr,OSSA2D}$) for both models are obtained and reported in Table 4. The corresponding analytical values $\alpha_{cr,anal} = N_{cr}/(P_1 + P_2)$ are also reported ($\alpha_{cr,anal,s}$ and $\alpha_{cr,anal,r}$ for the simplified and refined models respectively) and fit quite well with the numerical ones. Obviously, the lower values obtained with the simplified model when compared to the refined one, results from the fact that the rotational restraint of the main leg, as well as the continuity of the diagonals above the leg level, are disregarded.

Published in: Engineering Structures (2022), vol. 252, 113603
DOI: 10.1016/j.engstruct.2021.113603
Status: Postprint (Author's version)

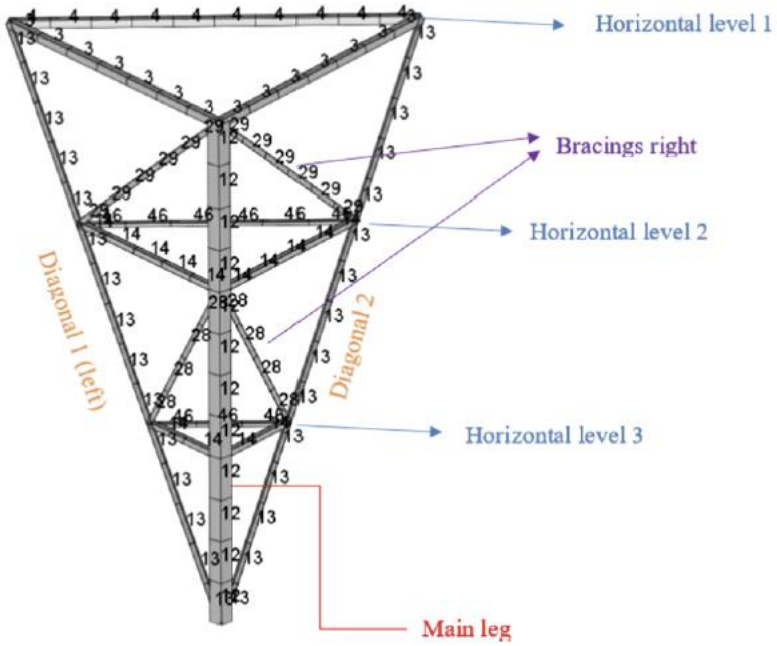

Fig. 15. Notations of the constitutive elements of the tower leg.

Table 3
Details of the leg members.

Member	CS code	Cross-section	Length [m]
Diagonal 1 (left)	13	75 × 75 × 4	6,00
Diagonal 2 (right)	13	75 × 75 × 4	6,00
Main leg	12	150 × 150 × 13	5,00
Horizontal level 2	14	60 × 60 × 4	1,827
Horizontal level 3	14	60 × 60 × 4	0,913

Table 4
Results obtained through the OSSA2D software and the analytical prediction models.

P_1 [kN]	P_2 [kN]	Simplified model		Refined model	
		$\alpha_{cr,OSSA2D}$ [-]	$\alpha_{cr,anal,s}$ [-]	$\alpha_{cr,OSSA2D}$ [-]	$\alpha_{cr,anal,r}$ [-]
30	0	1,19	1,21	1,33	1,33
30	15	0,80	0,80	0,90	0,89
30	20	0,72	0,72	0,81	0,80
30	30	0,59	0,60	0,67	0,67

Published in: Engineering Structures (2022), vol. 252, 113603
DOI: 10.1016/j.engstruct.2021.113603
Status: Postprint (Author's version)

Further numerical estimations of α_{cr} have been achieved for the transmission tower through an elastic instability analysis performed on the whole tower model, subjected to different actual external load combinations so as to vary the loading on the leg (in the exterior member and in the two diagonals). In Table 5, the obtained numerical results ($\alpha_{cr,FIN}$) are compared with the analytical ones for both proposed models.

Table 5
Results obtained for the whole tower model through FINELG and the analytical models.

Load combination	$P_1 + P_2$ [kN]	$\alpha_{cr,FIN}$ [-]	No of eigenmode	$\alpha_{cr,s}$ [-]	$\alpha_{cr,r}$ [-]	$\alpha_{cr,s}/\alpha_{cr,FIN}$ [-]	$\alpha_{cr,r}/\alpha_{cr,FIN}$ [-]
$G + W_y$	30,00	1,37	1	1,21	1,33	0,881	0,973
$G + W_x$	9,77	4,28	4	3,70	4,10	0,866	0,957
G_{tower}	1,83	23,99	12	19,75	21,84	0,823	0,910
Wx	7,15	6,42	1	5,06	5,60	0,788	0,872
Wy	33,05	1,48	1	1,10	1,21	0,740	0,818
Mean value	–	–	–	–	–	0,820	0,906

The safe character of the simplified approach may be seen. The refined design model in which the rotational restraint of the main leg member is taken into account gives better results than the simplified one as expected, but are still on the safe side. Obviously, one should compare the ultimate resistances and not only the critical ones in order to put a definitive judgement on the level of safety of the approach. By using the simplified model for the evaluation of the critical load, the leg slenderness is $\bar{\lambda} = \sqrt{\frac{2 \cdot 204,585}{N_{cr}}} = 3,363$, while, with the refined one, the slenderness slightly changes $\bar{\lambda} = 3,198$, but remains significantly high. With so high slenderness values, the ultimate resistance of the leg is almost equal to its critical resistance. So, in this specific situation, even if the comparisons between both models and FINELG would be done based on the ultimate resistances, the safe character would remain.

5.3. RECOMMENDATIONS OF THE NORMATIVE DOCUMENTS

As referred in the introduction, two main documents are used to design steel lattice transmission towers: EN 1993-3-1 and the CENELEC document EN 50341-1. In the latter, it is said that compression members shall be designed using the provisions of Annex G and Annex H of EN 1993-3-1, or in accordance with the provisions of Annex J.4 of EN 50341, only if full-scale tests are performed. In practice, full scale tests on towers are rarely performed and so the use of Annex J.4 of EN 50341 is rarely met. Accordingly, the remaining question is to see if the above- mentioned annexes of EN 1993-3-1 cover segment instability design check.

In fact, EN 1993-3-1, Annex H, clause H.3.7 recommends a buckling check of two members (one in each of two adjacent faces) against the algebraic sum of the loads in the two members connected by the diagonal brace over length L_{d4} (see Fig. 16) on the transverse axis, for cross bracing systems. For this case, the total resistance should be calculated as the sum of the buckling resistances of both members in compression.

Published in: Engineering Structures (2022), vol. 252, 113603
DOI: 10.1016/j.engstruct.2021.113603
Status: Postprint (Author's version)

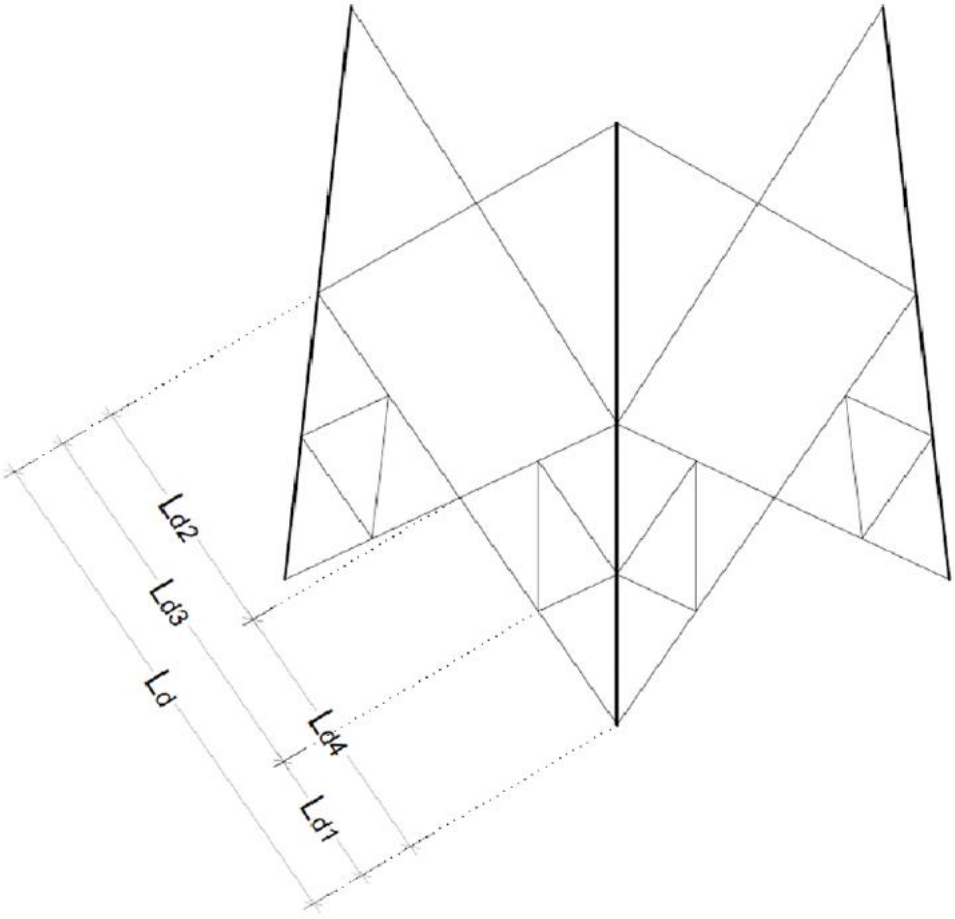

Fig. 16. Figure H.2(b) from EN 1993-3-1.

This design check looks to correspond to the simplified model proposed here. However, even if it seems clear for X bracings, it is not sufficiently clearly addressed for K bracings and therefore it is not sure that it is applied in practice. Besides that, in figure H.2, the member could also buckle along $L_{d,}$ what means that the two extremity points of the beam with length equal to L_{d4} are not laterally fixed, which leads to a more complex situation. Subsequently, the proposed models fill a gap in the provisions of the existing norms, clearly indicate the required check and recommend easy-to-apply design models.

5.4. APPLICATION OF THE DESIGN MODELS

In the following, an example illustrating the application of the design rules to the segment instability of the studied transmission tower is presented. The load sequence has been defined in Section 3, where 1,35*G* is applied first and then the wind load parallel to the cross arms is progressively increased 1,35α*W*y (α being the load factor).

Table 6 provides the values of the maximum compression loads and corresponding load factors evaluated by an elastic first order critical instability analysis and through analytical evaluations. The

Published in: Engineering Structures (2022), vol. 252, 113603
DOI: 10.1016/j.engstruct.2021.113603
Status: Postprint (Author's version)

segment instability mode that is illustrated in Fig. 4 appears far before the instability mode that would be detected according to EN 1993-3-1, i.e. the member instability of a single individual element (this instability takes place in diagonal 2 for α_{cr} = 1,66 and in the main leg for α_{cr} = 4,30), and therefore tends to be rather relevant.

Table 6
Load factors and critical loads for elastic critical instability.

Elastic critical instability	Buckling mode	Load factor α_{cr} [-]	Corresponding compression load [kN]	Level of accuracy
FINELG ($\alpha_{cr,FIN}$)	Segment	1,02	41,88	EN 1993-3-1: $\alpha_{cr,EC3}/\alpha_{cr,FIN}$ = 1,66
FINELG ($\alpha_{cr,FIN,diag}$)	Diagonal in between restraints – weak axis	1,66	66,30	
EN 1993-3-1 ($\alpha_{cr,EC3}$)		1,69	67,41	Proposed simplified model: $\alpha_{cr,anal,s}/\alpha_{cr,FIN}$ = 0,86 Proposed refined model: $\alpha_{cr,anal,r}/\alpha_{cr,FIN}$ = 0,96
Segment instability models:				
- Simplified model ($\alpha_{cr,anal,s}$)	Segment	0,87	36,19	Proposed refined model: $\alpha_{cr,anal,r}/\alpha_{cr,FIN}$ = 0,96
- Refined model ($\alpha_{cr,anal,r}$)	Segment	0,97	40,01	

Table 7 first provides the values of the actual ultimate compression loads and corresponding load factors that have been obtained through a GMNIA full geometrically and materially non-linear analysis considering all geometrical and material imperfections (by progressively increasing the value of α). They are compared to analytical evaluations evaluated by means of two proposed models using the European buckling curve d for the determination of the buckling reduction factors. Then the load factor has been derived numerically from a second order elastic analysis without initial imperfections to correspond to a force in the diagonals just equal to the ultimate one.

By performing a first order linear elastic analysis (α = 1,0), the compression force in the main leg of the segment equals 535,3 kN, while in diagonals 1 and 2 are 0,80 kN and 40,50 kN respectively. It is seen that those internal forces are much higher than the real ones obtained at the ultimate state, highlighting once again the influence of the second order effects on the response of the pylon and clearly indicating the need for their consideration in the structural analysis. Furthermore, it can be seen

Published in: Engineering Structures (2022), vol. 252, 113603
DOI: 10.1016/j.engstruct.2021.113603
Status: Postprint (Author's version)

that both prediction models for the segment instability working well and on the safe side, and although the simplified one is more conservative than the refined one, this doesn't set it inappropriate for use.

Table 7
Load factors and ultimate loads at the ultimate state.

Ultimate state	Buckling mode	Load factor α_u	Corresponding compression load [kN]	Level of accuracy
FINELG ($\alpha_{u,FIN}$)	Segment	0,66	(4,49 + 31,55) = 36,04	EN 1993-3-1: $\alpha_{u,EC3}/\alpha_{u,FIN}$ = unknown
EN 1993-3-1 ($\alpha_{u,EC3}$)	Diagonal in between restraints – weak axis	See comment below.[1]		Proposed simplified model: $\alpha_{u,anal,s}/\alpha_{u,FIN}$ = 0,86 Proposed refined model: $\alpha_{u,anal,r}/\alpha_{u,FIN}$ = 0,92
	Segment instability models:			
- Simplified model ($\alpha_{u,anal,s}$)	Segment	0,57	0,072·409,17 = 29,46	
Refined model ($\alpha_{u,anal,r}$)	Segment	0,61	0,079·409,17 = 32,32	

[1] This value cannot be evaluated through a second order elastic analysis, as the segment instability occurs before the diagonal buckles. But it may be seen that, when segment instability occurs ($\alpha_u = 0,66$), the force in diagonal 2 is equal to 31,50 kN while the ultimate buckling resistance between intermediate restraints according to EN 1993-3-1 (using buckling curve b for a slenderness 1,742) is equal to $N_{Rd} = \chi N_{pl} = 0,27 \cdot 204,59 = 55,24$ kN. Subsequently, the unconservative character of the present EN 1993-3 is seen to be rather significant.

6. Conclusions

An assessment of the current design approach used for lattice transmission towers has been performed through a full non-linear analysis using beam elements, considering relevant imperfections as well as geometrical and material non-linearities. From the numerical results, the following conclusions may be drawn.

Published in: Engineering Structures (2022), vol. 252, 113603
DOI: 10.1016/j.engstruct.2021.113603
Status: Postprint (Author's version)

The maximum load factor obtained by a 2nd order elastic analysis is higher than the critical one obtained by an elastic instability analysis. The reason is that the forces acting on the members in both cases differ, so affecting the member buckling load in the case of non- symmetrical cross-sections. Moreover, these effects are amplified with regard to the actual member support conditions (eccentricities for instance).

The second order effects should be taken into account in the analysis as they affect the global response of the tower and its ultimate state.

The initial design of the tower appears to be rather good in the case of application of the wind loads in one direction, but it is quite unconservative for the application of wind loads in the other direction. The reason is due to the development, in the second case, of an instability mode that is not properly recommended to be checked by the norms.

The new buckling instability mode named "segment instability" and involving more than one member has been detected, defined and characterised. It has been demonstrated that this instability mode is not properly covered by the present norms.

Two analytical models (a simplified and a refined one) for the prediction of the critical load of the new buckling mode have been proposed and validated numerically. The proposed design models are easy to apply, and fill the gap in the existing provisions of the European normative documents. The latter could be contemplated for a direct implementation of the future draft of the Eurocodes.

CRediT authorship contribution statement

Marios-Zois Bezas: Writing – original draft, Investigation, Software, Validation. **Jean-Pierre Jaspart:** Conceptualization, Supervision, Writing – review & editing. **Ioannis Vayas:** Writing – review & editing. **Jean-François Demonceau:** Methodology, Investigation.

Declaration of Competing Interest

The authors declare that they have no known competing financial interests or personal relationships that could have appeared to influence the work reported in this paper.

Acknowledgment

The work presented here is carried in the framework of a European Research project entitled ANGELHY "Innovative solutions for design and strengthening of telecommunications and transmission lattice towers using large angles from high strength steel and hybrid techniques of angles with FRP strips", with a financial grant from the Research Fund for Coal and Steel (RFCS) of the European Community. The authors gratefully acknowledge this financial support.

Published in: Engineering Structures (2022), vol. 252, 113603
DOI: 10.1016/j.engstruct.2021.113603
Status: Postprint (Author's version)

References

[1] EN 1993-3-1: Design of steel structures - Part 3-1: Towers, musts and chimneys. Tower and musts, Brussels, Comit´e Europeen de Normalisation (CEN), 2005.

[2] EN 1993-1-1: Design of steel structures - Part 1-1: General rules and rules for buildings, Brussels, Comite Européen de Normalisation (CEN), 2005.

[3] EN 1993-1-8: Design of steel structures - Part 1-8: Design of joints, Brussels, Comité Européen de Normalisation (CEN), 2005.

[4] EN 50341-1: Overhead electrical lines exceeding AC 1 kV - Part 1: General requirements - Common specifications, 2012.

[5] EN 1990: Eurocode - Basis of structural design, Brussels, Comite Européen de Normalisation (CEN), 2005.

[6] Klinger C, Mehdianpour M, Klingbeil D, Bettge D, Hacker R, Baer W. Failure analysis on collapsed towers of overhead electrical lines in the region Münsterland (Germany) 2005. Eng Fail Anal 2011;18(7):1873–83. https://doi.org/10.1016/j. engfailanal.2011.07.004.

[7] Albermani FGA, Kitipornchai S. Numerical simulation of structural behaviour of transmission towers. Thin-Walled Struct 2003;41(2-3):167–77. https://doi.org/ 10.1016/S0263-8231(02)00085-X.

[8] Silva JGS, Vellasco PCG, Andrade SAL, Oliveira MIR. Structural assessment of current steel design models for transmission and telecommunication towers. J Constr Steel Res 2005;61(8):1108–34. https://doi.org/10.1016/j.jcsr.2005.02.009.

[9] Jiang WQ, Wanga ZQ, McClure G, Wangc GL, Gengd JD. Accurate modelling of joint effects in lattice transmission towers. Eng Struct 2011;33:1817–27. https://doi.org/10.1016/j.engstruct.2011.02.022.

[10] Kitipornchai S, Albermani FGA, Peyrot AH. Effect of bolt slippage on ultimate behavior of lattice structures. J Struct Eng 1994;120(8). https://doi.org/10.1061/ (ASCE)0733-9445(1994)120:8(2281).

[11] Nuno J, Miller M, Kempner L. Historical perspective of full-scale latticed steel transmission tower testing. Electrical Transmission and Substation Structures 2012:313–22. https://doi.org/10.1061/9780784412657.027.

[12] Vlachakis K, Beyer A, Vayas I. Tragverhalten von Fachwerkmasten aus Winkelprofilen. Stahlbau 2021;90(6):425–40. https://doi.org/10.1002/stab. v90.610.1002/stab.202000059.

[13] Rao NP, Knight GMS, Mohan SJ. Studies on failure of transmission line towers in testing. Eng Struct 2012;35:55–70. https://doi.org/10.1016/j.engstruct.2011.10.017.

[14] prEN 1993-3-1: Design of steel structures - Part 3: Towers, musts and chimneys, Brussels, Comité Européen de Normalisation (CEN), 2020.

[15] Vayas I., Jaspart J.P., Bureau A., Tibolt M., Reygner S., Papavasiliou M., Telecommunication and transmission lattice towers from angle sections – the ANGELHY project, https://doi.org/10.1002/cepa, Ernst & Sohn, ce/papers, Special Issue: EUROSTEEL 2021 Sheffield — Steel's coming home, Vol. 4, Issue 2 – 4, 2021, pp. 210–217, 2021.

Published in: Engineering Structures (2022), vol. 252, 113603
DOI: 10.1016/j.engstruct.2021.113603
Status: Postprint (Author's version)

[16] Fischer R, Kießling F. Freileitungen: Planung, Berechnung, Ausführung. 4 Auflage. Springer Verlag; 2013.

[17] EN 50182: Conductors for overhead lines - Round wire concentric lay, Comité Européen de Normalisation (CEN), 2001.

[18] TOWER User's Manual – Version1 15.0, ©Power Line Systems Inc, 2017.

[19] EN 50341-2-4, Overhead electrical lines exceeding AC 1 kV - Part 2-4: National Normative Aspects (NNA) for Germany (based on EN 50341-1:2012), 2016.

[20] Tibolt M, Bezas M-Z, Vayas I, Jaspart J-P. The design of a steel lattice transmission tower in Central Europe, Ernst & Sohn, ce/papers, Special Issue: EUROSTEEL 2021 Sheffield — Steel's coming home, 2021;4(2–4): 243–248, https://doi.org/10.1002/cepa.1288, 2021.

[21] FINELG: Non-linear finite element analysis program, User's manual, Version 9.0, Greisch Ingeniere, 2003.

[22] de Ville de Goyet V., L'analyse statique non linéaire par la méthode des éléments finis des structures spatiales formées de poutres à section non symétrique, PhD thesis, University of Liege, 1989.

[23] Bezas M-Z, Demonceau J-F, Vayas I, Jaspart J-P. Experimental and numerical investigations on large angle high strength steel columns. Thin-Walled Struct 2021; 159C:107287. https://doi.org/10.1016/j.tws.2020.107287.

[24] Bezas M-Z. Design of lattice towers from hot-rolled equal leg steel angles. PhD thesis. University of Liege & National Technical University of Athens; 2021.

[25] Zhang L, Jaspart JP. Stability of members in compression made of large hot-rolled and welded angles. Université de Liège; 2013.

[26] EN 1991-1-4: Actions on structures- Part 1-4: General actions, Wind actions, Brussels, Comité Européen de Normalisation (CEN), 2005.

[27] Bezas MZ, Tibolt M, Jaspart JP, Demonceau JF. Critical assessment of the design of an electric transmission tower. In: 9th International Conference on Steel and Aluminium Structures, 3-5 July, Bradford UK, 2019.

[28] ANGELHY Deliverable 1.3, Report on analysis and design of 6 case studies, Research Program of the Research Fund for Coal and Steel ANGELHY, Grant Agreement Number: 753993, European Commission, Brussels, Belgium, 2019.

[29] Gardner L. Stability of steel beams and columns in accordance with Eurocodes and UK National Annexes, SCI publication P360, ISBN 978-1-85942-199-4, Berkshire, UK, 2011.

[30] Petersen C. Statik und Stabilitat der Baukonstruktionen (in German), ISBN 978-3-528-18663-0. Germany: Friedrich Vieweg & Sohn Verlag; 1982.

[31] OSSA2D: Finite element analysis program, User's manual, Version 3.4, University of Liege, 2020.